Formation of Ultrasharp Vertically Aligned Cu−Si Nanocones by a DC Plasma Process

K. L. Klein,[†,‡] A. V. Melechko,[†,‡] J. D. Fowlkes,[†,‡] P. D. Rack,[‡] D. K. Hensley,[†] H. M. Meyer, III,[§] L. F. Allard,[§] T. E. McKnight,[†] and M. L. Simpson*[,†,‡]

Molecular-Scale Engineering and Nanoscale Technologies Research Group, Oak Ridge National Laboratory, Oak Ridge, Tennessee 37831-6006, Department of Materials Science and Engineering, University of Tennessee, Knoxville, Tennessee 37996-2200, and Microscopy Microanalysis and Microstructures Group, Metals and Ceramics Division, Oak Ridge National Laboratory, Oak Ridge, Tennessee 37831-6064

Received: November 9, 2005; In Final Form: January 13, 2006

We report an effective method for the production of ultrasharp vertically oriented silicon nanocones with tip radii as small as 5 nm. These silicon nanostructures were shaped by a high-temperature acetylene and ammonia dc plasma reactive ion etch (RIE) process. Thin-film copper deposited onto Si substrates forms a copper silicide (Cu_3Si) during plasma processing, which subsequently acts as a seed material masking the single-crystal cones while the exposed silicon areas are reactive ion etched. In this process, the cone angle is sharpened continually as the structure becomes taller. Furthermore, by lithographically defining the seed material as well as employing an etch barrier material such as titanium, the cone location and substrate topography can be controlled effectively.

Introduction

High aspect ratio conical nanostructures are of significant interest because of their diverse applications including scanning probe microscopy tips,[1] gene delivery arrays,[2,3] and microfabricated field-emission sources.[4,5] However, the functionality of such devices depends on the control of the nanocone characteristics such as tip size, height, location, and chemical composition. Smaller tip sizes enhance the performance of many nanoscale devices such as improved resolution in scanning probe microscopy, damage-free delivery of materials through cell membranes for biological applications, and greater field enhancement at the tip for field-emission applications. Carbon nanofibers or nanotubes, grown catalytically by thermal chemical vapor deposition (CVD)[6,7] or by plasma-enhanced chemical vapor deposition (PECVD) methods,[8−10] are used commonly for such applications. However, other materials deserve exploration and may offer unique advantages such as robustness, greater uniformity, simpler fabrication, novel chemical functionality, and compatibility with semiconductor processing.

Conical nanostructures provide considerably more mechanical and thermal stability than their cylindrical counterparts because of their large bases while still affording the precision associated with small tip sizes and high aspect ratio. Nanoscale cones can be shaped out of numerous materials. Pure carbon conical nanostructures have been formed by the pyrolysis of hydrocarbons resulting in folded concentric graphene sheets,[11] and conical crystals have been discovered in the pores of glassy carbons.[12,13] Recently, efforts to generate graphitic nanocones on substrates by a catalytic growth approach have proven successful using microwave plasma CVD.[14−16] Furthermore, composite conical structures have been produced by dc PECVD, whereby cylindrical carbon nanofibers are encapsulated by precipitates of varying thickness.[17−19] Similar results have been reported for SiC nanowires covered in SiO_2.[20]

Conical nanomaterials can also be shaped by a substrate etching approach in a plasma environment. This type of process is capable of providing greater orientation control by the directionality of physical and chemical etching as well as greater height uniformity because the tips reside at the original surface of the substrate. Sharp nanotips have been fabricated conventionally by focused ion beam (FIB) milling of the substrate with a high degree of control.[21] The drawback to this method is that it is a serial process for producing conical structures on an individual basis. Other etching or sputter-induced methods, such as those reported by Hsu et al. and Fujomoto et al., provide an efficient parallel process but lack control over the nanotip location.[22,23] Being able to control the location, orientation, size, and shape of the nanocones in a deterministic way is necessary for many applications, but scalability of the process is also important.

In this work we present the fabrication of ultrasharp nanocones by a dc plasma process. Copper films deposited on a silicon substrate were subjected to plasma conditions similar to the PECVD growth of carbon nanofibers,[8] with increased plasma energy. However, this process yielded nanocone structures with an entirely different morphology, internal structure, and chemical composition. The self-assembled copper particles proved to be poor catalysts for carbon nanofiber growth but were instead excellent seed materials for the formation of silicon nanocones. This letter investigates the structure and mechanism of formation of these nanostructures as well as ways to control their synthesis deterministically. Furthermore, this study provides insight on the behavior of copper films and silicon substrates at elevated temperatures in a reactive ion etching environment, which is a subject of high interest for the semiconductor industry.[24−26]

* Corresponding author. Phone: (865)574-8588, fax: (865)574-1753, e-mail: SimpsonML1@ornl.gov.

[†] Molecular-Scale Engineering and Nanoscale Technologies Research Group, Oak Ridge National Laboratory.

[‡] Department of Materials Science and Engineering, University of Tennessee.

[§] Microscopy Microanalysis and Microstructures Group, Metals and Ceramics Division, Oak Ridge National Laboratory.

10.1021/jp0564997 CCC: $33.50
Published on Web 02/11/2006

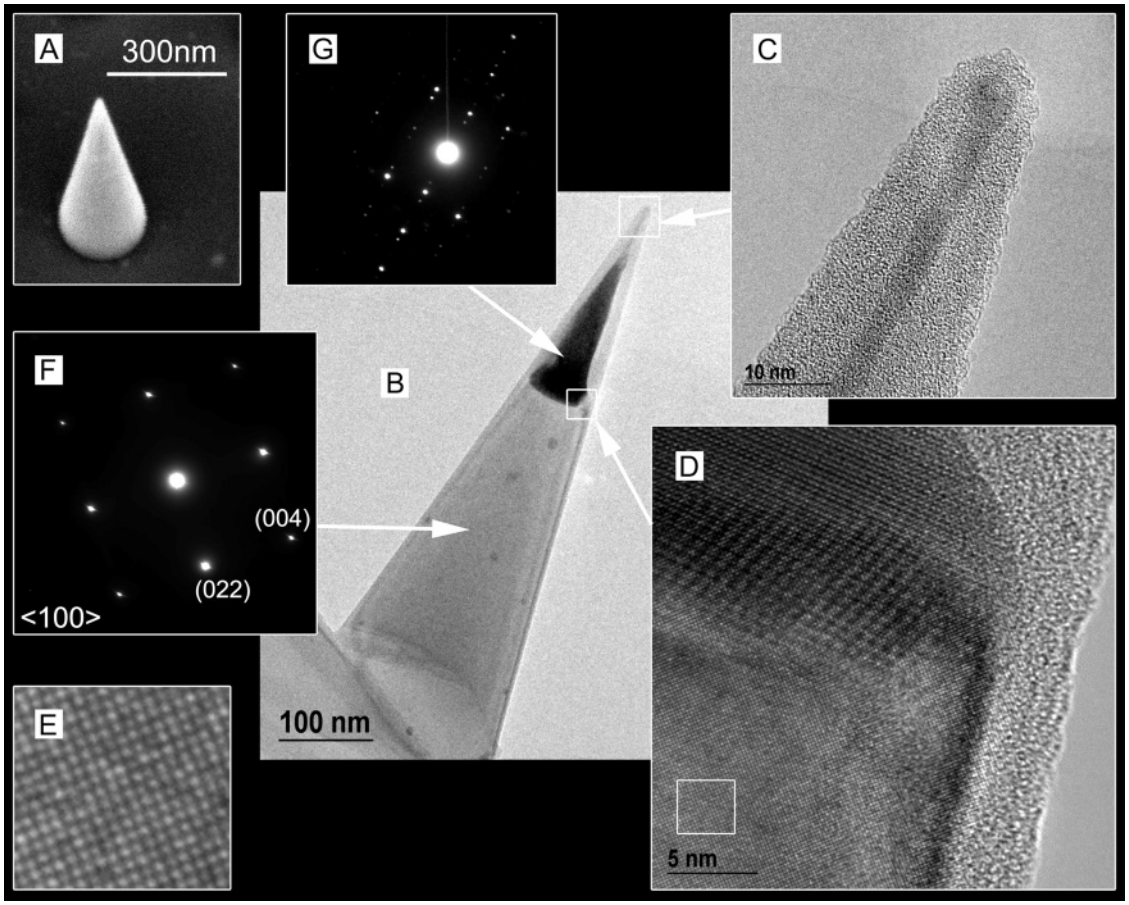

Figure 1. Image collage of a typical nanocone after a 105-min plasma process: (A) SEM image at a 30° tilt, (B) TEM profile image of a nanocone with a close-up (C) of the 10-nm tip and (D) tip−base interface with inset (E) of the Si lattice, diffraction patterns (F) from the single-crystal silicon base, and (G) crystalline Cu−Si tip.

Experimental Methods

For stochastic nanocone arrays, substrates were prepared by electron beam evaporation of 20-nm uniform Cu films at room temperature onto Si(100) and Si(111) n-type wafers. In the case of periodic nanocone arrays, 700-nm-diameter 150-nm-thick Cu dots were photolithographically defined at 5-μm intervals on the silicon substrate. Titanium was also applied as an etch-stop on some samples, in which case a 100-nm Ti layer was evaporated directly onto the Si substrate prior to Cu film deposition.

The Cu−Si nanocones were produced from a Cu-facilitated reactive ion etch process. In this process, the substrate described above was subjected to a dc glow discharge (setup described in detail elsewhere).[8,17] Upon a 2-min pretreatment at 700 °C and 2.5 Torr in an ammonia plasma, the continuous Cu thin film separated into alloyed Cu−Si nanoparticles on the surface, which served as seeds for the nanocone formation. In the case of Cu periodically patterned dot arrays, the pretreatment step was omitted because seed particles had been defined lithographically. Following seed particle formation, acetylene (C_2H_2) was introduced at 25 sccm into the chamber as a moderating agent. Without the moderating gas, the seed material as well as the nanocones would have been etched away within minutes. The samples were reactive ion etched for intervals of time ranging from 30 to 240 min. Optimal conditions required a plasma bias of 550−650 V at 150 mA.

The samples were first characterized by scanning electron microscopy (SEM) in a Hitatchi S-4700 and by scanning auger microprobe (SAM) in a PHI 680. Then the nanocones were transferred to lacey carbon coated beryllium grids and analyzed by high-resolution transmission electron microscopy (HRTEM; Hitatchi HF-2000) and by scanning transmission electron microscopy (STEM; Hitatchi HD-2000). The STEM's high sensitivity energy-dispersive X-ray spectroscopy (EDS) mapping capabilities were utilized to determine the elemental composite structure of the nanocones. In addition, X-ray diffraction (XRD) was performed on the as-evaporated Cu film, annealed, plasma pretreated, and reactive ion etched samples for comparison. Si(111) substrates were used for this experiment to avoid the overlap of the Si(220) peak with the high-intensity copper silicide peaks. For these data, a Philips X'Pert diffractometer was used to produce grazing incidence ω-2θ scans of the samples in order to probe the Cu−Si interface structure and composition. The Cu Kα (1.54 Å) X-rays were generated using a source excitation voltage of 45 kV and current of 40 mA. The divergence of the incident and diffracted beam was minimized using a 0.04 rad Soller slit. The rectangular X-ray beam was shaped using a 10-mm incident beam mask and a fixed slit of 1/8°. A beam attenuation optic was activated in the incident beam path to prevent detector saturation.

Results and Discussion

The dc plasma process described above transformed the surface topography of the substrate effectively. What was originally a silicon substrate covered with thin film copper transformed into a dense array of aligned ultra-sharp nanocones as shown in Figure 1A. Figure 1B−F shows a collage of HRTEM images and diffraction patterns from a typical nanocone after a 105-min process at optimal conditions. The central image,

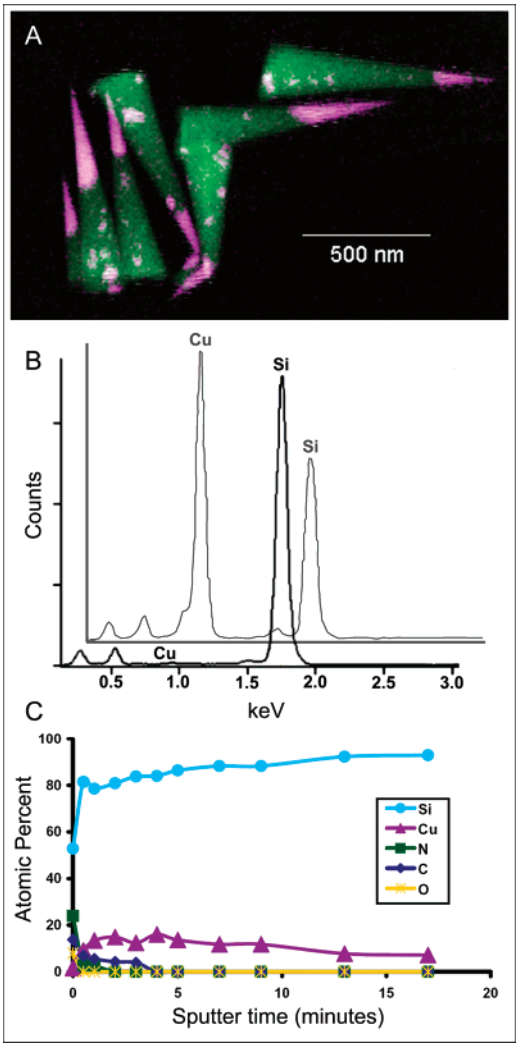

Figure 2. Chemical analysis of typical nanocones: (A) EDS elemental map of several cones showing copper in pink (light) and silicon in green (dark), (B) point EDS from a cone base overlaid on an EDS spectra from a cone tip, and (C) auger depth profile of a nanocone.

Figure 1B, shows a base segment of lighter contrast and a tip segment of darker contrast. The entire structure is encapsulated by a few nanometers of amorphous material, thickening at the top of the structure. The HRTEM close-up of the intersection of the base and tip segments (Figure 1D) reveals the Si lattice (inset Figure 1E) overlapping with the Cu_xSi lattice. The electron diffraction pattern in Figure 1F reveals that the nanocone bases are single-crystal Si with the same ⟨100⟩ orientation as the substrate. For the (022) planes, a d spacing of 1.93 Å was measured, corresponding to a lattice parameter of 5.45 Å, which agrees with literature values.[27] The nanocone tips are a crystalline form of copper silicide as given by the diffraction pattern in Figure 1G.

The EDS map shown in Figure 2A gives a visual illustration of the elemental distribution for several nanocones after a 240-min process. The nanocones are predominately silicon with sharp Cu-rich tips and occasional Cu-rich aggregates within the silicon crystal lattice. Point EDS of a nanocone base segment (Figure 2B) shows that the ratio of copper to silicon is less than 1%. The minor C and O peaks originate from elements in the amorphous outerlayer. The tip EDS analysis in Figure 2B shows an atomic ratio of 38.7% Si to 61.3% Cu. Because a compound of Cu_2Si is not thermodynamically stable, it seems most probable that the tip crystal is of the form Cu_3Si with the additional Si contribution originating from the outerlayer. This outer amorphous coating encapsulating the nanocone is composed of a mixture of C, N, O, and Si, as shown by the scanning auger microprobe results plotted in Figure 2C. After briefly sputtering the nanocone-covered substrate with argon in the SAM, the outerlayer was removed completely, resulting in a purely Cu and Si nanocone underneath. This silicon-rich amorphous outerlayer is a result of sidewall deposition of condensed species from the plasma.[18,19] The carbon and silicon contained in the outer coating may play a crucial role in protecting the sidewalls of the conical structure during the plasma process and is believed to be facilitated by the presence of carbon-rich acetylene gas.

A time evolution of the nanocone structure demonstrated by three stages in the formation process is displayed in Figure 3. After 30 min in the dc plasma environment, examination of the sample revealed emerging stump-like structures shown in Figure 3A. These "pre-cone" structures were relatively evenly spaced less than a 1 μm apart and stood between 400 and 600 nm tall. Most of the pre-cone structures contained a copper-rich tip particle of variable size between 20 and 200 nm. All of the structures had a silicon base segment of roughly the same size of 200 nm tall, shown in Figure 3B and C. The cone angle varied from 22° to 26°.

Subjecting the Cu-covered silicon substrate to a longer plasma process of 105 min resulted in the uniform cone structures shown in Figure 3D. The nanocones were not much larger than the pre-cones from the 30 min plasma process, standing only 600−700 nm tall; however, each structure had a sharp cone angle ranging from 18° to 21° and a very small tip diameter. Further analysis by TEM revealed that the copper silicide particles located at the tip had molded into the conical structure sharing a distinct (often angled) grain boundary with the silicon (Figure 3E).

Investigating further, the substrate was exposed to an even longer dc plasma process of 240 min, which resulted in ultrasharp nanocones with an angle of 9−14°, shown in Figure 3F−I. Additionally, there was a doubling in height of the structures to 1.5 μm. The copper silicide tips, covered by a few nanometers of amorphous substance, were only 10 nm in diameter. Thus, as the nanocones became taller, they sharpened continually. The presence of a subarray of smaller secondary cones should also be noted in the longer process, as observed in Figure 3F. These secondary cones are thought to be the result of Cu seed material sputtering and redeposition because they are considerably shorter than the original cones. Perhaps once the nanocone is fully formed with a sharp cone angle, the copper material at the cone tip becomes thinned and heated because of the field effects and is consequently more easily sputtered. The sputtered material is then redeposited nearby on the substrate and serves as the seed for secondary cone formation.

Grazing incidence X-ray diffraction of the substrate surface gives further evidence of the morphology and phase changes occurring during the cone formation process. As can be seen from the SEM image and corresponding spectra in Figure 4A, the initial Cu film evaporated onto the Si(111) substrate gives broad Cu(111) and Cu(200) peaks at 2θ angles 43.37° and 50.53°, respectively, indicative of a fine-grained polycrystalline film. After annealing at 700 °C, the Cu peaks become sharper, indicative of a larger grain size in the aggregating film shown in Figure 4B. Comparing the integrated peak intensities to a polycrystalline copper standard also reveals some degree of texture in the annealed nanoparticle film, with a preference for Cu(200). During a 2-min exposure to the ammonia plasma environment at 700 °C, the copper particles react with the silicon

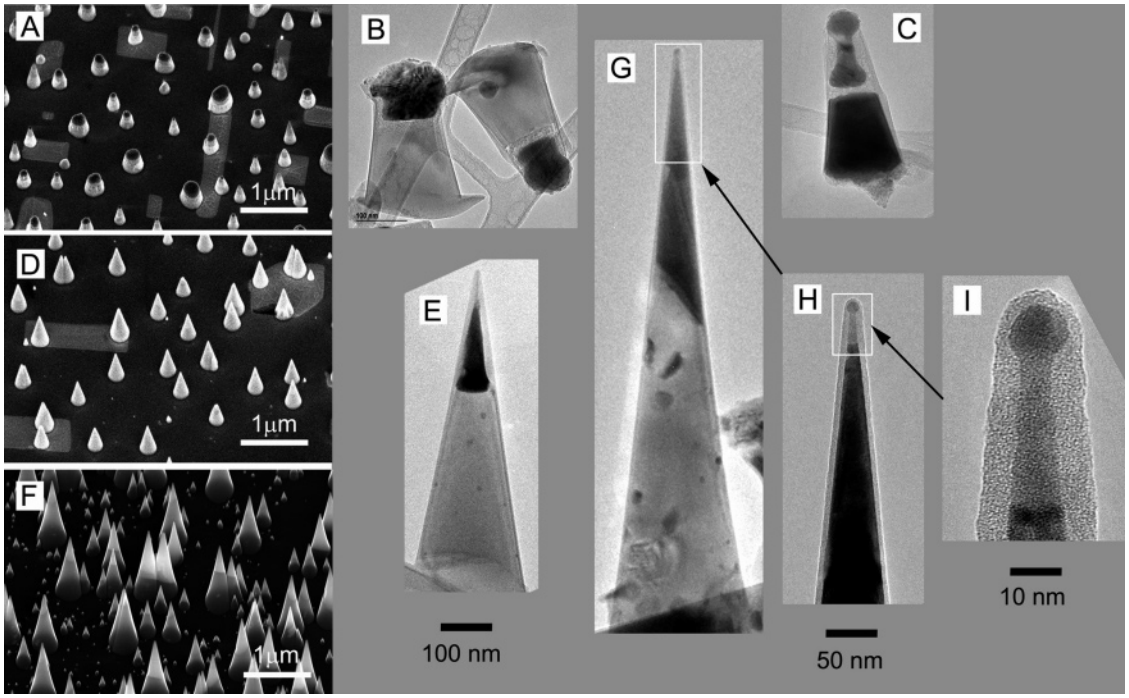

Figure 3. Time evolution of nanocone formation shown at three stages. Stage one, a 30-min plasma process: (A) SEM image at a 30° tilt, (B and C) TEM images of early pre-cone formation. Stage two, a 105-min plasma process: (D) SEM image at a 30° tilt and (E) TEM image. Stage three, a 240-min plasma process: (F) SEM image at a 30° tilt and (G) TEM image of a typical nanocone with insets (H) and (I) of the sharpened tip. Scale bars are 1 μm for A, D, and F; 100 nm for B, C, E, and G; 50 nm for H; 10 nm for I.

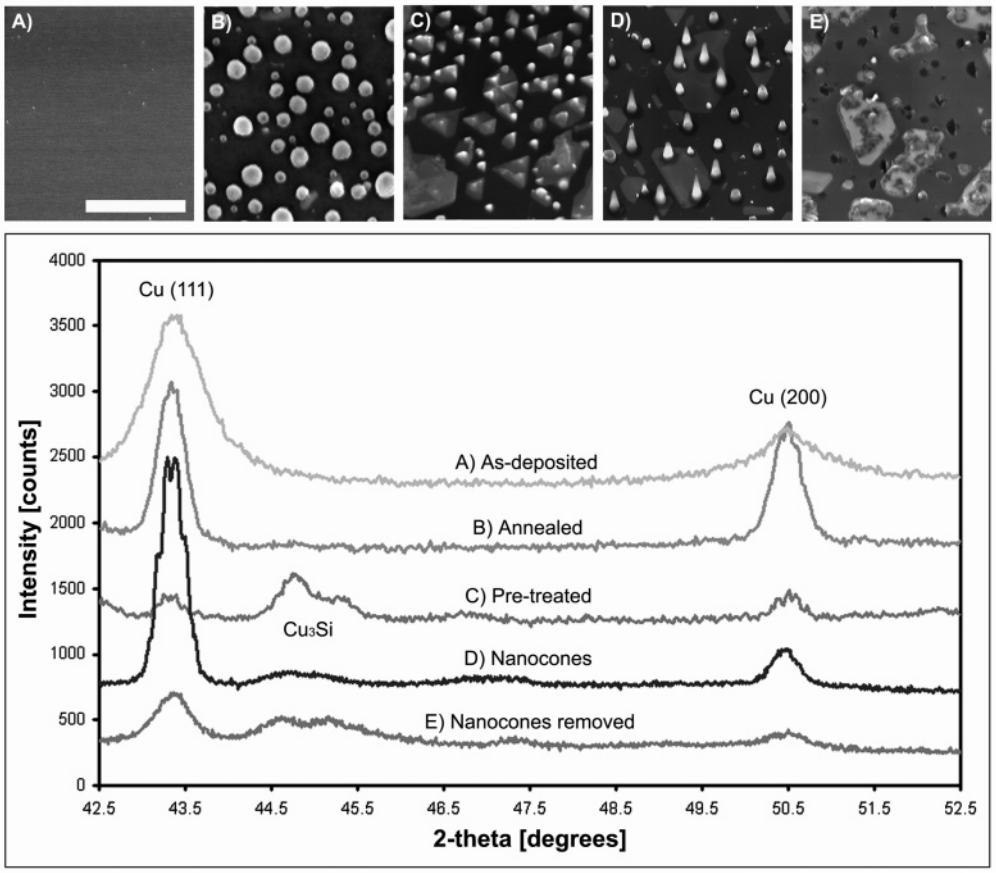

Figure 4. SEM images at 30° tilt and corresponding grazing incidence XRD Cu Kα scans of sequential stages in the cone formation process: (A) as-deposited 20-nm Cu film on a Si(111) substrate, (B) sample annealed at 700 °C for 2 min, (C) plasma pretreated sample, (D) 120-min plasma processed sample with nanocones, and (E) substrate after nanocones were removed. All SEM images were taken at the same magnification, and the scale bar in A is 2 μm.

substrate to form a hexagonal Cu_3Si phase shown by the appearance of peaks at 2θ 44.61° and 45.17° in Figure 4C corresponding to the $(11\bar{2}0)$ and $(10\bar{1}1)$ reflections, respectively.[25] At this stage the copper reflection intensity is reduced

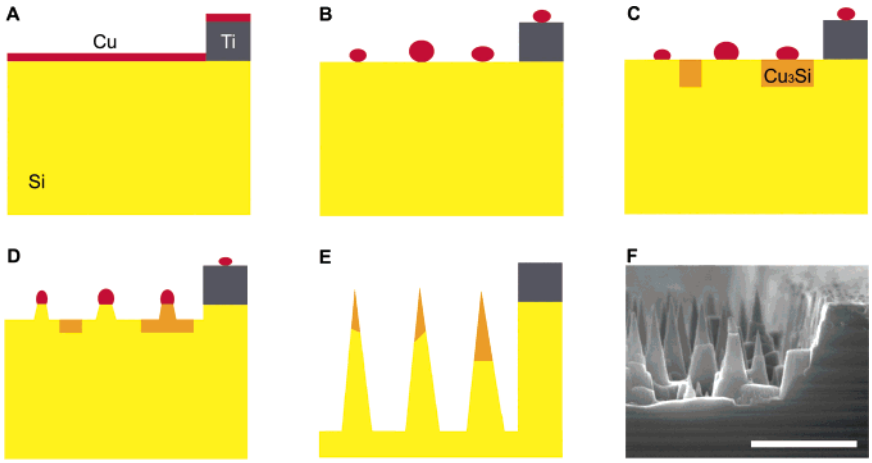

Figure 5. Model of the cone formation process: (A) evaporation of patterned 100-nm Ti film and continuous 20-nm Cu film, (B) heating of the substrate to 700 °C to form Cu nanoparticles, (C) plasma pretreatment and formation copper silicide, (D) plasma etching of the substrate surface forming pre-cone structures, (E) continued plasma etching and interdiffusion of Cu and Si at the nanocone tips (F) cross-sectional SEM image of the experimental nanocone result of step (E), scale bar is 1 μm.

because of its partial conversion to silicide. After cones are formed beneath the Cu particles from prolonged interaction with the plasma, the Cu(111) and (200) peaks re-emerge, geometrically suppressing the silicide reflections from the surface as shown in Figure 4D. To verify the location of the Cu particles, we removed the cones from the substrate by scraping, and the XRD result in Figure 4E is analogous to the pretreated sample, 4C. It is our belief that the cones formed in 4D are more similar to the pre-cones mentioned earlier than the sharp nanocones. Insufficient plasma energy most likely delayed sharpening of the cones, leaving round copper particles at their apex similar to the images in Figure 2A−C.

A model of the cone formation process is presented in Figure 5. Here Ti is employed as an etch barrier material to mark the original substrate level and control the location of the nanocones. Formation of the cones is prohibited where the Ti layer is defined on the Si substrate. After Ti is deposited, copper is evaporated over the entire surface (A). At elevated temperatures the Cu film breaks into nanoparticles (B), which react with the substrate under plasma conditions forming Cu_3Si on the silicon surface (C). This silicide formed at the Cu−Si interface acts as a barrier for further copper diffusion[26] and the copper particles remain, shielding the underlying substrate from the plasma. As time passes, the Si is etched away at a rate of ~4 nm/min and the pre-cones are formed (D). With even more time, the copper particles themselves slowly etch away diminishing in size and sharpening the tip as the nanocones become taller (E). In turn, the field at the tips of the cones is enhanced as their aspect ratio increases and localized heating occurs. More silicide is formed at the same time the copper at the very tip is sputtered away. The result is a high aspect ratio array of silicon nanocones with copper silicide at their tips as shown in F. In the regions where the Ti film served as a buffer layer, the surface remained unetched by plasma. Beneath the titanium, the original substrate level can be seen, which is expectedly the same height as the nanocone formations.

It is believed that the nanocones presented in this paper are the result of a reactive ion etch process occurring at the substrate. Reactive ion etching is the likely explanation because there appears to be characteristic evidence of both physical and chemical etching. To begin with, there is a high degree of directionality in the process resulting in an anisotropic, physical etching of the cones out of the substrate. Hence, the portion of the substrate covered by the copper seed material (serving as an etch mask) is preserved.[22,23] Furthermore, there is sufficient energy in the plasma to induce sputtering of the substrate, indicated by the Si sidewall deposition and the formation of secondary cones.[23] However, there are additional aspects characteristic of a dry chemical etch such as selectivity, favoring the etching Si over Cu or Ti, the high-pressure plasma environment, and the relatively fast etch rate. In addition, the nanocones did not exhibit any faceting on their external surfaces. It should also be noted that substrate doping did not affect the etch rate significantly.

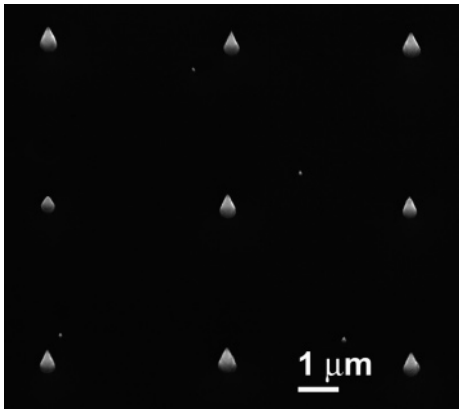

Figure 6. SEM image at 30° tilt of a 5-μm pitch periodic nanocone array produced from photolithographically defined Cu dots.

Recent success in forming periodic arrays of the nanocones is presented in Figure 6. By lithographically defining the location of the Cu seed particles, the nanocone location is controlled effectively. This concept, coupled with the etch selectivity for Si versus Ti, can be utilized to pattern the substrate such that nanocones will only form in the absence of a Ti film and the presence of Cu seed particles. This results in a deterministic process to form nanocone arrays of variable heights and spatial organization.

Conclusions

This letter describes a method of producing ultrasharp nanocones via an acetylene and ammonia dc plasma process. Thorough characterization of these structures has revealed that the nanocones consist of single-crystal silicon bases with the same orientation as the substrate and crystalline copper silicide tips 10 nm in diameter. We have concluded that the mechanism

for the formation of these interesting structures is reactive ion etching of the silicon substrate facilitated by copper seed particles. In this process, the nanocones become sharper as they increase in height. Furthermore, it has been shown that by patterning the seed and etch barrier materials the location of the nanocones can be predetermined.

Acknowledgment. M.L.S. acknowledges support from the Material Sciences and Engineering Division Program of the DOE Office of Science under contract DE-AC05-00OR22725 with UT-Battelle, LLC, and K.L.K. acknowledges support from the Center for Nanophase Materials Sciences (CNMS) Research Scholar Program. Additional support was provided by the Defense Advanced Research Projects Agency (DARPA) under Contract no. DE-AC05-00OR22725 and by the National Institute for Biomedical Imaging and Bioengineering under assignment 1-R21-EB004066-01. Scanning Auger Microanalysis was sponsored by the Assistant Secretary for Energy Efficiency and Renewable Energy, Office of FreedomCAR and Vehicle Technologies, as part of the High Temperature Materials Laboratory User Program, ORNL, managed by UT-Battelle, LLC, for the US Department of Energy under contract no. DE-AC05-00OR22725. We thank Pam Flemming, Teri Subich, and Darrell Thomas for film deposition and lithography.

References and Notes

(1) Cui, H.; Kalinin, S. V.; Yang, X.; Lowndes, D. H. *Nano Lett.* **2004**, *4*, 2157.

(2) McKnight, T. E.; Melechko, A. V.; Griffin, G. D.; Guillorn, M. A.; Merkulov, V. I.; Serna, F.; Hensley, D. K.; Doktycz, M. J.; Lowndes, D. H.; Simpson, M. L. *Nanotechnology* **2003**, *14*, 551.

(3) McKnight, T. E.; Melechko, A. V.; Hensley, D. K.; Mann, D. G. J.; Griffin, G. D.; Simpson, M. L. *Nano Lett.* **2004**, *4*, 1213

(4) Guillorn, M. A.; Yang, X.; Melechko, A. V.; Hensley, D. K.; Hale, M. D.; Merkulov, V. I.; Simpson, M. L.; Baylor, L. R.; Gardner, W. L.; Lowndes, D. H. *J. Vac. Sci. Technol., B* **2004**, *22*, 35.

(5) Merkulov, V. I.; Lowndes, D. H.; Baylor, L. R. *J. Appl. Phys.* **2001**, *89*, 1933.

(6) Cassell, A. M.; Raymakers, J. A.; Kong, J.; Dai, H. J. *J. Phys. Chem. B* **1999**, *103*, 6484.

(7) Li, W. Z.; Xie, S. S.; Qian, L. X.; Chang, B. H.; Zou, B. S.; Zhou, W. Y.; Zhao, R. A.; Wang, G. *Science* **1996**, *274*, 1701.

(8) Merkulov, V. I.; Lowndes, D. H.; Wei, Y. Y.; Eres, G.; Voelkl, E. *Appl. Phys. Lett.* **2000**, *76*, 3555.

(9) Chen, Y.; Wang, Z. L.; Yin, J. S.; Johnson, D. J.; Prince, R. H. *Chem. Phys. Lett.* **1997**, *272*, 178.

(10) Ren, Z. F.; Huang, Z. P.; Xu, J. W.; Wang, J. H.; Bush, P.; Siegal, M. P.; Provencio, P. N. *Science* **1998**, *282*, 1105.

(11) Krishnan, A.; Dujardin, E.; Treacy, M. M. J.; Hugdahl, J.; Lynum, S.; Ebbesen, T. W. *Nature* **1997**, *388*, 451.

(12) Gogotsi, Y.; Dimovski, S.; Libera, J. A. *Carbon* **2002**, *40*, 2263.

(13) Gogotsi, Y.; Libera, J. A.; Kalashnikov, N.; Yoshimura, M. *Science* **2000**, *290*, 317.

(14) Tsai, C. L.; Chen, C. F.; Wu, L. K. *Appl. Phys. Lett.* **2002**, *81*, 721.

(15) Mani, R. C.; Li, X.; Sunkara, M. K.; Rajan, K. *Nano Lett.* **2003**, *3*, 671.

(16) Zhang, G. Y.; Bai, X. D.; Jiang, X.; Wang, E. G. *Science* **2004**, *303*.

(17) Merkulov, V. I.; Melechko, A. V.; Guillorn, M. A.; Lowndes, D. H.; Simpson, M. L. *Appl. Phys. Lett.* **2001**, *79*, 2970.

(18) Cui, H.; Yang, X.; Meyer, H. M.; Baylor, L. R.; Simpson, M. L.; Gardner, W. L.; Lowndes, D. H.; An, L.; Lui, J. *J. Mater. Res.* **2005**, *20*.

(19) Klein, K. L.; Melechko, A. V.; Rack, P. D.; Fowlke, J. D.; Meyer, H. M.; Simpson, M. L. *Carbon*, in press, 2005.

(20) Lin, M.; Loh, K. P.; Boothroyd, C.; Du, A. Y. *Appl. Phys. Lett.* **2004**, *85*, 5388.

(21) Vasile, M. J.; Biddick, C.; Huggins, H. *Appl. Phys. Lett.* **1994**, *64*, 575.

(22) Hsu, C. H.; Lo, H. C.; Chen, C. F.; Wu, C. T.; Hwang, J. S.; Das, D.; Tsai, J.; Chen, L. C.; Chen, K. H. *Nano Lett.* **2004**, *4*, 471.

(23) Fujimoto, Y.; Nozu, M.; Okuyama, F. *J. Appl. Phys.* **1995**, *77*, 2725.

(24) Istratov, A. A.; Weber, E. R. *J. Electrochem. Soc.* **2002**, *149*, G21.

(25) Chromik, R. R.; Neils, W. K.; Cotts, E. J. *J. Appl. Phys.* **1999**, *86*, 4273.

(26) Lee, C. S.; Gong, H.; Liu, R.; Wee, A. T. S.; Cha, C. L.; See, A.; Chan, L. *J. Appl. Phys.* **2001**, *90*, 3822.

(27) Batchelder, D. N.; Simmons, R. O. *J. Chem. Phys.* **1964**, *41*, 2324.